Manual Onboard Methods of Orbit Determination

PETER BIELKOWICZ*
Air Force Institute of Technology, Wright-Patterson Air Force Base, Ohio
AND
ROGER C. HORRIGAN† AND RICHARD C. WALSH‡
Air Force Satellite Control Facility, Sunnyvale, Calif.

This paper reviews some manual, onboard-orbit-determination methods for use when electronic equipment fails. It outlines the methods developed at the AF Institute of Technology; only brief remarks are given to the other procedures. Each of the methods discussed is based on the results of manual onboard range measurements performed at 3 or 5 points of the orbit at short time intervals. From altitude (range) increments it is possible to determine for the midpoint on the orbit the planetocentric range, the magnitude of the vehicle's velocity V, and its inclination α to the local horizon. All in-plane orbital parameters and the value of the minimum range can be expressed and plotted as functions of $(V/V_c)^2$ and α. Another method enables the navigator to read the values of orbital parameters, that of the period and the time to perifocus directly from the few charts presenting these magnitudes as functions of the range increments Δh_1 and Δh_2 hence its name: Δh method. Its applications are however limited to small ranges and low-eccentricity orbits. Using a relatively small number of charts the onboard orbit determination may be completed in 15-25 min, including the observational time. Possible extension of the latter method to high eccentricity and long-range orbits is discussed, and recommendations are made for the further development of hardware and methods.

Nomenclature

a = semimajor axis
e = eccentricity of the orbit
E = eccentric anomaly
h_i = altitude above the surface of a planet
H = angular momentum per unit of mass
Δh_i = range or altitude increment $= r_i - r_{i+1}$
M = mean anomaly
n = mean angular velocity
r = planetocentric range (from midpoint of measurements)
r_p = $a(1 - e)$ for an ellipse and $a(e - 1)$ for a hyperbola
R = mean radius of a planet
t_i = time at the point r_i
V_c = speed in a circular orbit of the radius r
V_{co} = sea or ground level circular velocity
θ = true anomaly
μ = gravity constant of a planet
τ_c, τ = periods of circular and elliptic orbits, respectively
ψ = angle measured by stadimeter
α = angle of the velocity vector with the horizontal at measurement midpoint

Introduction

AT present, onboard manual navigation methods may be considered as a desirable safety precaution to be used in the event of a communication failure on a spacecraft. In the future they will become an absolute necessity. A take-off from the far side of the moon would require that the safe check of the orbit be performed by the spacecraft navigator. A similar need would occur in the case of a close approach to Mars or Jupiter. Assuming a temporary failure of electronic equipment, this check would have to be made by simple manually operated instruments and a slide rule or small calculating machine. The principles of the orbit determination are those long established in celestial mechanics. Their application, however, differs considerably from the procedure used by a ground observer who knows his own coordinates and is not required to complete all computations in a few minutes. To permit determination of the spacecraft's orbital parameters the orbit should be close to a conic section, and the spacecraft window should produce only a small refraction error. The navigator has such simple instruments as a stadimeter and a space sextant and is able to measure at least three distances, h_1, h_2, and h_3 from the planet. The mean value of the equatorial and polar radius is used as the planet's radius, $R = (R_e + R_p)/2$. Usually it is impossible for the navigator to perform a simultaneous position fix, so he determines it between the range measurements. The determination of the orientation parameters will be discussed briefly.

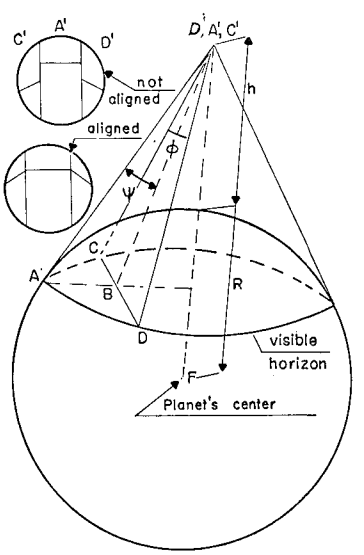

Fig. 1 Stadimeter's geometry.

Presented as Paper 70-159 at the AIAA 8th Aerospace Sciences Meeting, New York, January 19–21, 1970; submitted February 20, 1970; revision received November 20, 1970.

* Professor of Aero-Space Engineering. Associate Fellow AIAA.
† Major USAF. Member AIAA.
‡ Capt. USAF, Chief of Satellite Operations, Satellite Test Center.

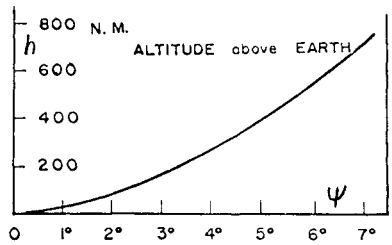

Fig. 2 Stadimeter's calibration curve.

The stadimeter (Fig. 1) can be used only at a short distance from a planet: up to 2500 naut miles from the Earth, or up to 700 naut miles from the moon. For larger distances a space sextant is used. For Earth, the thickness of the atmosphere is added to the mean radius, $R' = R + 14.9$ naut miles.[4] The stadimeter measures the curvature of the horizon circle and converts it into the altitude of the observer. It uses a triple split image field with a center scanning prism A'. The side fields C' and D' become oriented at points C and D on the visible horizon circle of the planet. The angle Φ between $C'C$ and $D'D$ is fixed and known. The central prism A' scans in a plane normal to CD until an alignment is obtained (Fig. 1), then the line $A'A$ intersects the horizon circle, and the angle ψ is read from the instrument. With ψ, Φ and R known, the distance $h = r - R$ is obtained from the geometry of the figure as a function of ψ. Figure 2 represents the calibration of the stadimeter for the Earth.

Velocity and Inclination Method

This rapid method of onboard orbit determination is based on the estimation of the velocity of the vehicle and of its inclination α to the local horizontal from three or five observations, each yielding an altitude h_i. The magnitude of velocity computed at the middle point of five or three observations is determined from[1]

$$V^2 = V_c^2 + \dot{r}^2 + r\ddot{r} \tag{1}$$

Hence the magnitudes of r, $\dot{r}$, and $\ddot{r}$ should be determined first. In the case of only three observations we consider $r = r_2$ as a reference value, $\dot{r}_2 = \dot{r}$, $\ddot{r}_2 = \ddot{r}$. By using the stadimeter we find r_1, r_2, r_3 at the times t_1, t_2, t_3. Assume $t_3 > t_2 > t_1$. Then $r_1 - r_2 = \Delta h_1 = -\dot{r}(t_2 - t_1) + \ddot{r}(t_2 - t_1)^2/2$,

$$r_3 - r_2 = -\Delta h_2 = \dot{r}(t_3 - t_2) + \ddot{r}(t_3 - t_2)^2/2 \tag{2}$$

$$\dot{r} = -[\Delta h_1(t_3 - t_2)^2 + \Delta h_2(t_2 - t_1)^2][(t_2 - t_1)(t_3 - t_2)(t_3 - t_1)]^{-1} = -\Delta h_1(t_3 - t_2)(t_2 - t_1)^{-1} \times (t_3 - t_1)^{-1} - \Delta h_2(t_2 - t_1)(t_3 - t_2)^{-1}(t_3 - t_1)^{-1} \tag{3}$$

$$\ddot{r} = 2\Delta h_1(t_2 - t_1)^{-1}(t_3 - t_2)^{-1} - 2\Delta h_2(t_3 - t_2)^{-1}(t_3 - t_1)^{-1} \tag{4}$$

If the time intervals are equal, then

$$\dot{r} = -(\Delta h_1 + \Delta h_2)/2\Delta t \tag{5}$$

$$\ddot{r} = (\Delta h_1 - \Delta h_2)/(\Delta t)^2 \tag{6}$$

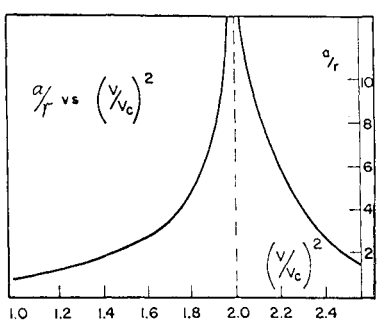

Fig. 3 Semimajor axis vs normalized velocity.

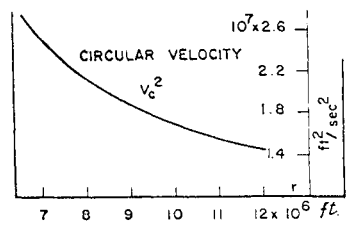

Fig. 4 Circular velocity vs selenocentric range for the moon.

The truncation error[2] can be considerably reduced by retaining five terms in the serial expansions of r_1, r_2, r_4, r_5, which are now performed with respect to the middle value $r = r_3$, $\dot{r} = \dot{r}_3$, and $\ddot{r} = \ddot{r}_3$. The total observation time is doubled. Assuming equal time intervals, we obtain four equations:

$$\begin{aligned}
r_1 - r_3 &= (r_1 - r_2) + (r_2 - r_3) = \Delta h_1 + \Delta h_2 = \\
&\quad \dot{r}(2\Delta t) + (\ddot{r}/2)4(\Delta t)^2 - (\dddot{r}/6)8(\Delta t)^3 + (\ddddot{r}/24)16(\Delta t)^4 \\
r_2 - r_3 &= \Delta h_2 = -\dot{r}\Delta t + (\ddot{r}/2)(\Delta t)^2 - (\dddot{r}/6)(\Delta t)^3 + \\
&\quad (\ddddot{r}/24)(\Delta t)^4 \\
r_4 - r_3 &= -\Delta h_3 = \dot{r}\Delta t + (\ddot{r}/2)(\Delta t)^2 + (\dddot{r}/6)(\Delta t)^3 + \\
&\quad (\ddddot{r}/24)(\Delta t)^4 \\
r_5 - r_3 &= r_5 - r_4 + r_4 - r_3 = -\Delta h_4 - \Delta h_3 = \\
&\quad \dot{r}2\Delta t + (\ddot{r}/2)4(\Delta t)^2 + (\dddot{r}/6)8(\Delta t)^3 + (\ddddot{r}/24)16(\Delta t)^4
\end{aligned} \tag{7}$$

Solving the system (7) with respect to $\dot{r}$ and $\ddot{r}$,

$$\dot{r} = [\Delta h_1 + \Delta h_4 - 7(\Delta h_2 + \Delta h_3)]/12\Delta t \tag{8}$$

$$\ddot{r} = [\Delta h_4 - \Delta h_1 + 15(\Delta h_2 - \Delta h_3)]/12(\Delta t)^2 \tag{9}$$

We substitute these values into the Eq. (1). If $V^2 > 2V_c^2$ the orbit is a hyperbola. If $V^2 < 2V_c^2$, it is an ellipse. The semimajor axis a is determined from $a = r/[2 - (V/V_c)^2]$ for an ellipse, or $a = r/[(V/V_c)^2 - 2]$ for a hyperbola.[3] Given $(V/V_c)^2$, one may use Fig. 3 to determine a/r. The same graph serves all planets and covers both elliptic and hyperbolic orbits. Values of the local circular velocity V_c can be read from the auxiliary graphs. In Fig. 4 the values of V_c^2 vs r for the moon are plotted. The other orbital parameters are obtained as the functions of $(V/V_c)^2$ and α, where $\sin\alpha = \dot{r}/V$. The curves of constant α are plotted vs $(V/V_c)^2$ for e, e^2, true anomaly θ and the minimum planetocentric distance $r_p = a(1 - e)$. (See, e.g., Fig. 5). The same graphs are valid for the Earth, the moon, and all planets.

We can determine e from

$$e^2 = 1 - H^2/\mu a, \text{ for an ellipse or} \tag{10a}$$

$$e^2 = 1 + H^2/\mu a, \text{ for a hyperbola} \tag{10b}$$

where the angular momentum $H = rV\cos\alpha$. Since $V_c^2 = \mu/r$,

$$e^2 = 1 - (V/V_c)^2[2 - (V/V_c)^2]\cos^2\alpha \tag{11a}$$

$$e^2 = 1 + (V/V_c)^2[(V/V_c)^2 - 2]\cos^2\alpha \tag{11b}$$

for an ellipse and a hyperbola, respectively. In Fig. 5, for a given value of α, if $(V/V_c)^2 < 1$, the vehicle is on the ellipse

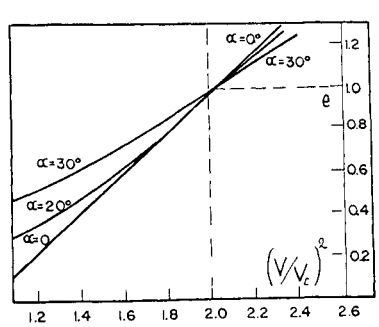

Fig. 5 Eccentricity vs normalized velocity.

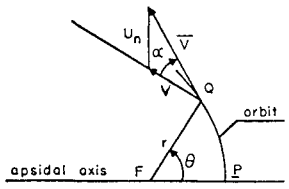

Fig. 6 Components of orbital velocity.

between the apofocus and the minor axis. If $2 > (V/V_c)^2 > 1$, it is on the elliptic path between the perifocus and the end of the minor axis. If $\dot{r} < 0$, it is approaching the perifocus. Direction of the apsidal axis can be defined in the planetocentric inertial system by a unit vector $\hat{P}$ pointing at the perifocus and making an angle θ (the true anomaly) with the known position vector $\bar{r}$ of the vehicle. At any point on the conic path, described in a central gravity field, the velocity is the vector sum of two components of constant magnitude: $u_n = e\mu/H$, which has a constant direction remaining normal to the apsidal axis, and $v = \mu/H$, which is normal to the radius vector of a moving point. From Fig. 6, we obtain $u_n \sin\theta = V \sin\alpha$, $u_n \cos\theta = V \cos\alpha - v$, hence

$$\tan\theta = V \sin\alpha(V \cos\alpha - \mu/h)^{-1} = (V/V_c)^2 \sin\alpha \cos\alpha[(V/V_c)^2 \cos^2\alpha - 1]^{-1} \quad (12)$$

The plot of θ vs $(V/V_c)^2$ is shown in Fig. 7.

The velocity at the perifocus of the orbit can be expressed as $V_p = v + u_n$. The perifocal distances for an orbit are given by $r_p/r = (a/r)(1 - e)$ for an ellipse, and $r_p/r = (a/r)(e - 1)$ for a hyperbola. Hence

$$r_p/r = [2 - (V/V_c)^2]^{-1}\{1 - [1 - (V/V_c)^2 \times (2 - V^2/V_c^2) \cos^2\alpha]^{1/2}\}$$
$$r_p/r = [(V/V_c)^2 - 2]^{-1} \times \{[1 + (V/V_c)^2(V^2/V_c^2 - 2) \cos^2\alpha]^{1/2} - 1\} \quad (13)$$

for an ellipse and for a hyperbola, respectively. Both cases of the system (13) are represented on the same graph (Fig. 8). If $\alpha = 0$ but $V \neq V_c$, the vehicle is at the apse of its orbit; indeed, for an elliptic orbit, $r_p/r = \{1 - [1 - 2(V/V_c)^2 + (V/V_c)^4]^{1/2}\}[2 - (V/V_c)^2]^{-1} = \{1 - [(V/V_c)^2 - 1]\}[2 - (V/V_c)^2]^{-1} = 1$; hence $r = r_p$ for $V > V_c$ and $r = r_a$ for $V < V_c$. If $\alpha = 0$ and $V/V_c = 1$, then identically $r \equiv r_p$, and the orbit is a circle. In order to find the time elapsed between the perifocus and the midpoint, the value of the eccentric anomaly at $r = r_3$ should be found from

$$e \sin E = r\dot{r}/(\mu a)^{1/2}; \quad e \cos E = 1 - r/a, \dot{r} = V \sin\alpha$$
$$\tan E = V \sin\alpha(a/\mu)^{1/2}/(a/r - 1) = (V/V_c) \sin\alpha[2 - (V/V_c)^2]^{1/2}/[(V/V_c)^2 - 1] \quad (14)$$

and E is plotted vs $(V/V_c)^2$ and α. The graph is valid for all planets. From the known E the time to perifocus is computed and plotted for each planet individually, since n depends on $\mu = k^2M$.

Safe Orbit Check

The save-check of the orbit by using the $(V/V_c)^2$, α method requires only three charts: a) calibration of the stadimeter: h vs ψ; b) $V_c^2 = \mu/r$ vs r (optional); and c) r_p/r vs $(V/V_c)^2$ and α. The procedure is:

1) at time intervals $\Delta t = 5$ min or $\Delta t = 15$ min, perform five observations yielding (if stadimeter is used) ψ_1, ψ_2, ψ_3, ψ_4, ψ_5;

2) from the graph read $h_1, \ldots,$ and determine $\Delta h_1 = h_1 - h_2$, $\Delta h_2 = h_2 - h_3$, $\Delta h_3 = h_3 - h_4$, $\Delta h_4 = h_4 - h_5$;

3) compute $r = R + h_3$, $\dot{r} = [\Delta h_1 + \Delta h_4 - 7(\Delta h_2 + \Delta h_3)]/12\Delta t$, $\ddot{r} = [\Delta h_4 - \Delta h_1 + 15(\Delta h_2 - \Delta h_3)]/12(\Delta t)^2$;

4) from a corresponding chart read or compute $V_c^2 = \mu/r$;

5) find $s^2 = V^2 = V_c^2 + \dot{r}^2 + r\ddot{r}$ and $(V/V_c)^2 = 1 + (\dot{r}^2 + r\ddot{r})/V_c^2$;

6) find $\sin\alpha = \dot{r}/V$ and α;

7) use the chart r_p/r vs $(V/V_c)^2$ and find r_p/r from the curve of constant α. Charts have been prepared for $\Delta\alpha = 2.5°$.

8) Check $r_p - R = (r_p/r)r - R \lesseqgtr 0$.

The navigator may then determine other orbital parameters from the remaining graphs and equations. The accuracy of this method depends on the accuracy of the observations and on the truncation error. The time required for this procedure is 5 observations, 20 min; computations, ~8 min.

Tabular and Altitude Charts Methods

Kollsman Instrument Corporation built the stadimeter and developed a tabular solution for determination of e, period, and t_1 (time from the first observation to the perifocus) from the three measured altitudes. This method requires, however, a separate table for each possible nautical mile of h_2. If a spacecraft were in an orbit between the altitudes 90 and 250 naut miles it would be necessary to carry at least 160 tables. Universal Technology Corporation developed a different method using an overlay which consists of concentric ellipses representing the curves of constant e (Fig. 9). The center point lies on the 45° diagonal representing the value of h_2. It corresponds to a circular orbit at this altitude. Vertical and horizontal axes represent the altitudes h_1 and h_3. Each graph, therefore, corresponds to a particular value of h_2. Normals to the diagonal are the $\Delta\tau$ lines, representing the increments $\Delta\tau$ from the period τ_c of the circular orbit having the radius $R + h_2$. Time t_1 from perifocus to the first stadimetric measurements is found from graphs for each h_2. The method requires, however, an iteration between the graphs. It also requires a number of the overlay charts, one for each value of h_2.[4-6]

Δh Method

The method of altitude increments (Δh) uses as variables[4]: $\Delta h_1 = h_1 - h_2 = r_1 - r_2$, $\Delta h_2 = h_2 - h_3 = r_2 - r_3$. Only three altitudes are required. The values of V, $\dot{r}$, $\ddot{r}$ are not computed so the truncation error is avoided. This error, however, affects the computation of the eccentric anomaly

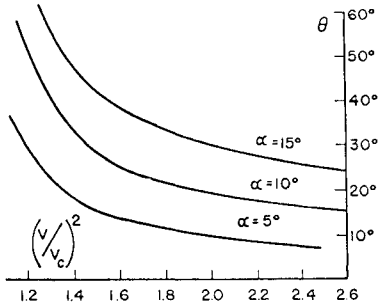

Fig. 7 True anomaly vs normalized velocity.

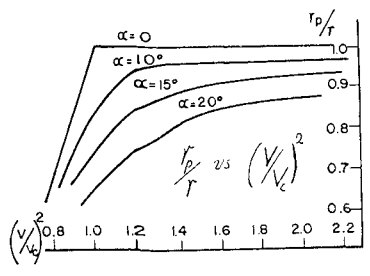

Fig. 8 Periapsis radius r_p vs normalized velocity.

E from Kepler's equation for an elliptic orbit:

$$E = M + e\sin M + (e^2/2)\sin 2M + (e^3/8) \times (\sin 3M - \sin M) \quad (15)$$

The series is convergent only for $e < 0.663$. Hence the method cannot be used for high eccentricity orbits like, for example, an Earth-moon trajectory.

Analysis of this method is briefly outlined. We have r_1, r_2, r_3 at time t_1, t_2, t_3,

$$r_1 = a(1 - e\cos E_1); \quad E_1 - e\sin E_1 = M_1 = n(t_1 - T) \quad (16a)$$

$$r_2 = a(1 - e\cos E_2) \quad (16b)$$

$$E_2 - e\sin E_2 = M_2 = n(t_2 - T), \; r_3 = a(1 - e\cos E_3) \quad (16c)$$

$$E_3 - e\sin E_3 = M_3 = n(t_3 - T) \quad (16d)$$

where T is the time of passage through perifocus. It is assumed, obviously, that the orbit is an ellipse. Subtracting, we obtain

$$\Delta h_1 = r_1 - r_2 = ae(\cos E_2 - \cos E_1) \quad (17a)$$

$$\Delta h_2 = r_2 - r_3 = ae(\cos E_3 - \cos E_2) \quad (17b)$$

$$n(t_2 - t_1) = n\Delta t = E_2 - E_1 - e(\sin E_2 - \sin E_1) \quad (17c)$$

$$n(t_3 - t_2) = n\Delta t = E_3 - E_2 - e(\sin E_3 - \sin E_2) \quad (17d)$$

where $n = (\mu/a^3)^{1/2}$. So we have four equations containing five unknowns: E_1, E_2, E_3, a, and e. Let us fix e; then we can eliminate E_1, E_2, E_3 from the system. Finally, we obtainonly one equation of the form

$$F(a,e,\Delta h_1,\Delta h_2,\Delta t) = 0 \quad (18)$$

where e is a fixed value, and a is a variable function of Δh_1 and Δh_2. So apparently this method would not present a great advantage over the overlay (h_1,h_2,h_3) method. Smith and Schehr,[4] however, discovered that for small eccentricity orbits in the close vicinity of a planet the plots $\Delta h_1 = f(\Delta h_2)$, which represent constant e curves, do not depend on the variation of a. This was confirmed later by Horrigan and Walsh.[3] Hence, in the case of Earth, for $R + 80 < a < R + 170$ naut miles and for $e < 0.1$, $\partial F/\partial a \cong 0$, and one graph would serve all values of h_2 (Fig. 10) satisfying the restricting conditions which are usually fulfilled by parking orbits. The graph represents a family of constant-e curves. The origin is at the point where $\Delta h_1 = \Delta h_2 = 0$ and represents a circular orbit at any altitude h_2. It would be possible on the same graph to plot the curves of constant E. Indeed, by eliminating E_2, E_3, and e we may have $F_1(a,E_1,\Delta h_1,\Delta h_2,\Delta t) = 0$, but this method was not applied in the present paper, and only the limits of the regions for E are shown on the working graphs. The values Δh_1 and Δh_2 define a point on the graph; this point determines e and shows in which quadrant E lies (Fig. 10). If $|\Delta h_1|$ and $|\Delta h_2|$ are both less than 1 naut miles the orbit is considered as circular.

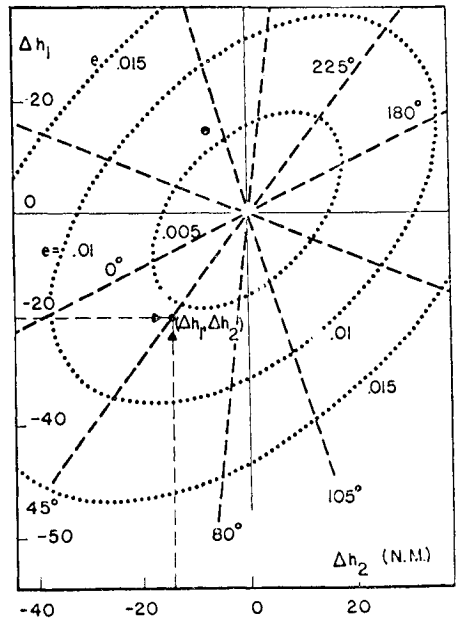

Fig. 10 Eccentricity as function of altitude differences with altitude.

The period τ_c of a circular orbit of a radius $r = R + h$ is given by the expression $\tau_c = 2\pi R^{3/2}[1 + (\frac{3}{2})(h/R) + (\frac{3}{8})(h/R)^2 + \ldots]/\mu^{1/2}$. For a lunar orbit it becomes $\tau_c = 108.55\,[1 + (\frac{3}{2})(h/R) + (\frac{3}{8})(h/R)^2]$ (minutes). On Fig. 11 the method of finding the period of an elliptic orbit is shown. The values of h_2 are marked on the diagonal at 45° to the axes h_1 and h_3. The entering arguments are h_1 and h_3. Then the distance from the point (h_1,h_3) to the normal at h_2 on the diagonal is measured and converted into time $\Delta\tau$ in minutes by using the enclosed time-scale. $\Delta\tau$ is multiplied by a correction factor K and added to τ_c corresponding to $h = h_2$.

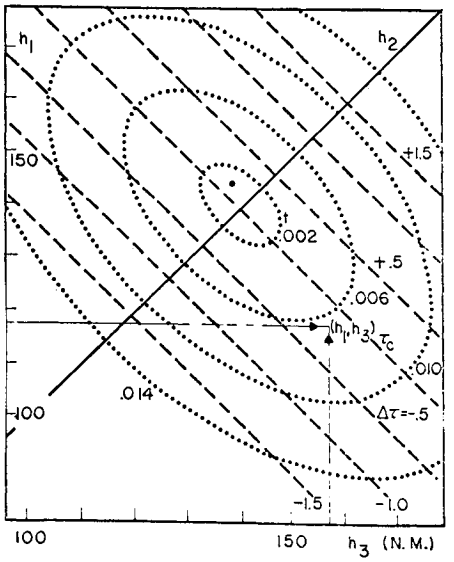

Fig. 9 Determination of eccentricity and period with altitude.

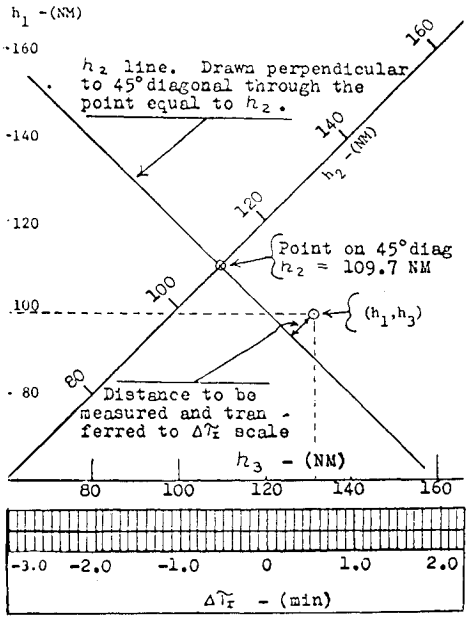

Fig. 11 Example of period determination.

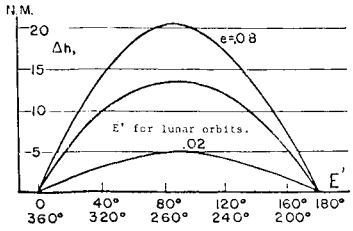

Fig. 12 Eccentric anomaly as function of altitude difference and eccentricity, Δh_1 and e.

For Earth, $K_{E15} = 1$, if $\Delta t = 15$ min; or $K_{E5} = 8.2$, if $\Delta t = 5$ min. For the moon, $K_{M15} = 2.4$, if $\Delta t = 15$ min; or $K_{M5} = 18.9$, if $\Delta t = 5$ min. $\Delta\tau$ assumes a negative or positive sign depending on the position of (h_1,h_3) with respect to the normal to the diagonal. The period of the orbit is $\tau = \tau_c \pm K\Delta\tau$.

In Fig. 12, Δh_1 is plotted vs E_1, but for reasons of symmetry E_1 was replaced by E', which is the eccentric anomaly at time $t' = t_1 + \Delta t/2$, $\Delta t = t_2 - t_1$; E' was called the eccentric anomaly factor. The quadrant to which E' belongs has already been determined from Fig. 10. In Fig. 13, the family of lines of constant e yields the values of t_1/τ for E_1. The time t_p till the next perifocus passage is, therefore, known: $t_p = \tau - t_1 = \tau[1 - t_1/\tau]$. The minimum orbital altitude occurs at the perifocus, where $h_p = r_p - R = a(1 - e) - R = [\tau^2\mu/4\pi^2]^{1/3}(1 - e) - R$; and h_p can be determined from Fig. 14, where the curves of constant τ are plotted vs e.

The time of the safe-orbit check includes the observation time $= 2\Delta t = 10$ min + computation and chart reading leading to determination of h_p. The total time is about 17–18 min.

The orientation parameters are determined by combining four star-horizon angle measurements with the geometric parameters already determined. These measurements are taken with the hand-held space sextant; they consist of two "shots" on each of two stars. Usually a 5-min interval is used between two angle measurements for each star. Then the orbital inclination i and the right ascension α of the ascending node are graphically determined as functions of the minimum co-altitudes of the two stars. The true anomaly of the ascending node can be calculated from the known true anomaly of the spacecraft at the time of the star-horizon angle measurement.

Further investigation of the manual navigation problem was accomplished at AFIT[3] with the objective of consolidating and extending the previously developed techniques and procedures with hopes of coming up with a flexible, general manual navigation system. The Δh method was extended to highly eccentric ellipses such as the translunar phase of the Apollo type mission. It was demonstrated that the constant-e curves on Δh_1 vs Δh_2 plots h_1, h_2 remain unchanged for $(\Delta a)/a < 0.03$ for low-e orbits. Therefore, for low-altitude, near-circular orbits one graph is sufficient to estimate e for all values of a. This is not exactly true for high-e orbits, where graphs of constant e must be prepared for different values of a (Fig. 15). Curve sensitivity to changes in a is much more severe in this region. Also, in order to separate the overlapping curves, Δt must be significantly increased.

Analysis

Horrigan and Walsh[3] also performed an error analysis of numerical differentiation of range measurements to obtain the

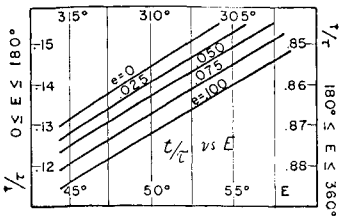

Fig. 13 Determination of the time to perifocus.

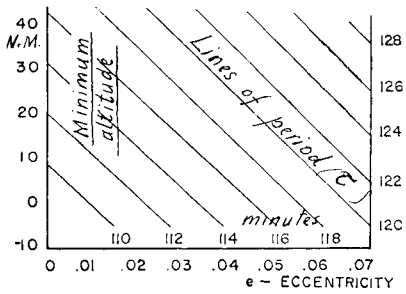

Fig. 14 Minimum orbital altitude above the moon as function of eccentricity and period.

geometric orbital elements, and investigated the possibility of using differential correction as a manual navigation technique. Whereas each of these held some promise, as has been seen for low-altitude, near-circular orbits, none was found to be flexible enough to be incorporated in a general manual navigation system due to a combination of unacceptable error effects and/or the need for excessive numbers of graphs and computations in the midcourse trajectory region.

Up to this point, it had been tacitly assumed that only discrete (separated in time) measurements were available for use in a manual navigation system. All computational procedures were based upon this assumption. It then occured to the investigators that the problem was indeed two-sided. On one side, measurements had to be performed to provide the input to the second side; the orbit determination computational procedures. Most work had been done on the second side of the problem, whereas the first had been virtually ignored. The question was asked, "In what form can the input measurements be cast to allow more flexible orbit determination procedures to be employed?" The answer was obvious. The three-dimensional (3-D) position fix has been the most important, and most sought after input to general, explicit orbit determination procedures for centuries. Manual navigation must be as simple as possible, yet retain the capability of defining any orbit or trajectory with sufficient accuracy to insure the safety of the spacecraft crew. Therefore, a general, two-body explicit approach utilizing position fixes seemed to be the next logical course to pursue.

The 3-D position fix involves, in its simplest form, two star-central body angular measurements coupled with a means to determine spacecraft radial distance from that central body. The equations involved are nonlinear and impractical for manual computations. Considerable simplification results, however, if one of the selected stars is Polaris, the North Star. If the second star is on the celestial equator, the right ascension and declination of the vehicle can be determined without resorting to the solution of the nonlinear set mentioned above. If, for some reason, Polaris is not available, some simplification results from a third star sighting. The three-star fix has been analyzed and found to be

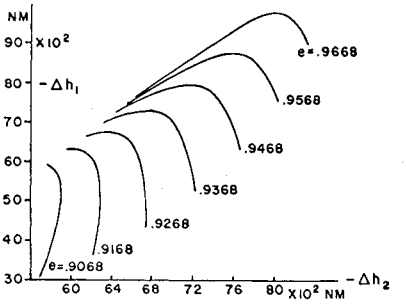

Fig. 15 Extension of Δh method for high eccentricity orbits (α = 107,000 naut miles, Δt = 60 min).

a suitable alternate procedure, although it requires the tabulation of possible three star sets to facilitate the solution of a linear set of equations. The authors believe that the Polaris method is the key to manual position fixing in space, particularly in the midcourse region, where extreme accuracy is not usually required. Further work in this area is necessary to determine the effect of Polaris' slight deviation from the pole position, especially in the near-planet region where the highest attainable accuracy is needed.

The simultaneous measurement requirement would be only a slight inconvenience to the spacecraft navigator. Once a "common" time has been established (say, at the time of the range measurement) a series of measurements, which may or may not bracket the common time, must be made to allow the use of some form of interpolation formula (e.g., Bessel's interpolation formula) to interpolate or extrapolate the measurements to the desired time. (If the range measurement time is chosen as the common time, the series of measurements would be star-central body, of course.)

Many well known orbit determination schemes were investigated. Most were eliminated from consideration due to the computational load imposed, e.g., by Battin's solution, which employs Lambert's theorem and requires a double iteration step[7] or mathematical inaccuracies due to the approximation of some quantity, e.g., the Herrick-Gibbs method, which utilizes numerical differentiation to obtain velocity at the midpoint of a set of position vectors.[1] The most promising computational procedure investigated[1] was the pure Gibbsian approach, which requires no iterations or approximations to obtain the elements of a two-body trajectory. Three position fixes are input, and through vector analysis the complete orbit is determined. A further advantage lies in the fact that the time between fixes is not required. This procedure can be accomplished by hand, but a small, battery-operated digital computer would be desirable. The Gibbs method was tested using data from a precision translunar trajectory generated by NASA. The output orbital elements were within 0.01% of the quoted values. This appeared very promising, but, of course, such accuracy is only attainable with extremely precise position fixing. In any case, the Gibbsian method seems to make nearly optimum use of position fix information.

Conclusions

The general conclusions drawn from this study of manual onboard orbit determination are:

1) for low-eccentricity, low-altitude orbits, many promising techniques are applicable;

2) none of these techniques, with the exception of the use of complete 3-D position fixes and something like the Gibbsian approach, seems to be flexible enough to be incorporated in a general manual navigation system;

3) the methods and procedures selected, therefore, are tied to the type mission to be flown;

4) to develop a general system, further work in software and hardware is necessary (hardware should be developed to support the best explicit computational scheme available).

References

[1] Baker, R. M., Jr., *Astrodynamics*, Computer Sciences Corporation, Los Angeles, Calif., 1967.

[2] Bielkowicz, P., "Charts and Diagrams for Fast Estimation of Orbital Elements," 1963–1965, Air Force Institute of Technology, Wright-Patterson Air Force Base, Ohio.

[3] Horrigan, R. and Walsh, R., "Manual Astronaut Navigation," MA. Thesis, 1969, Air Force Institute of Technology, Wright-Patterson Air Force Base, Ohio.

[4] Schehr, R. R. and Smith, P. J., "Manual Astronaut Navigation: Apollo Mission Applications," MA. thesis, June 1968, Wright-Patterson Air Force Base, Ohio

[5] Mills, J. and Silva, R., *Operational Computation Techniques*, Universal Technology Corp., Dayton, Ohio, 1968.

[6] Silva, Robert M. et al., "The Air Force Space Navigation Experiment on Gemini (DOD/NASA Gemini Experiment D-9, Gemini IV and VII Flights)," TR AFAL-TR-66-289, 1966, Air Force Avionics Lab., Research and Technology Div., Wright-Patterson Air Force Base, Ohio.

[7] Webber, A. et al., "Space Position Fixing Techniques, Phase II," Technical Documentary Rept. AFAL-RTD-ITR-1, 1967, Air Force Avionics Lab., Research and Technology Div., Wright-Patterson Air Force Base, Ohio.